Oral presentation | Data science and AI
Data science and AI-I
Wed. Jul 17, 2024 4:30 PM - 6:30 PM Room C

[9-C-04] Weight-Sharing Mode Decomposition Model Based on CNN for Unsteady Flows

*Yosuke Shimoda[1], Naoya Fukushima[1] (1. Tokai University)

Keywords: Mode Decomposition, Machine Learning, Convolutional Neural Network, Weight-Sharing Model, Unsteady Flow

Twelfth International Conference on Computational Fluid Dynamics (ICCFD12), Kobe, Japan, July 14-19, 2024

Weight-Sharing Mode Decomposition Model Based on CNN for Unsteady Flows

Y. Shimoda*, and N. Fukushima*
Corresponding author: y-shimoda@fuji.tokai-u.jp
*Tokai University, Kitakaname, Hiratsuka, Kanagawa, Japan

Abstract: To perform mode decomposition of complex flow fields, such as turbulence, we develop Weight-sharing CNN Mode Decomposition Model. By utilizing a common decoder with weight sharing, the model extracts multiple decomposed flow fields, thereby reducing the number of model layers and parameters. The array of the latent variables mapped from the original flow fields are labeled with the mode numbers. The decomposed flow fields are then obtained from the labeled modes using the shared decoder. The number of parameters of a shared decoder in the Model with n modes is reduced to $1/n$ compared to n decoders in a conventional model. This study applies the model to the two-dimensional flow around two parallel cylinders, at Reynolds number, $Re_D = U_\infty D/\nu = 100$, as an example of complex flows. The model demonstrated the ability to obtain decomposed flow fields with different characteristics using a single decoder for each mode. For the Model with 16 modes, training costs were reduced by approximately 64.4% per epoch compared to conventional models where each mode has its own decoder.

Keywords: Mode Decomposition, Machine Learning, Convolutional Neural Network, Weight-Shared, Unsteady Flows.

1 Introduction

Understanding, predicting, and controlling flow phenomena are crucial for improving the performance of various thermal fluid devices, contributing significantly to solving environmental and energy issues. In the field of fluid mechanics, numerous studies are conducted using various theoretical, numerical, and experimental methods. With the continuous development of computers, computational algorithms, measurement instruments, and measurement technologies, it is now possible to obtain large quantities of flow field data both numerically and experimentally through methods such as Direct Numerical Simulation (DNS) and Particle Image Velocimetry (PIV). Mode decomposition, which extracts potential and important features from these vast amounts of flow field data, is a valuable tool for deepening our understanding of flows. Common mode decomposition methods widely used in fluid mechanics include Proper Orthogonal Decomposition (POD) and Dynamic Mode Decomposition (DMD) [1, 2].

Recently, deep learning, which is increasingly utilized across various fields, has the potential to be a nonlinear analysis method by employing nonlinear activation functions. Flows, particularly turbulence, exhibit strong nonlinearity and multiscale phenomena, making them challenging to understand. Consequently, deep learning is expected to be one of the most powerful methods for understanding flow phenomena, especially turbulence, and its application in fluid mechanics is expanding. For instance, several studies have applied deep learning to mode decomposition of flow fields. Murata *et al.* constructed a Mode Decomposing Convolutional Neural Network Autoencoder (MD-CNN-AE) using Convolutional Neural Networks (CNN) and Autoencoders (AE), decomposing the velocity fields around a two-dimensional cylinder into two modes [3]. Wu *et al.* investigated the reconstruction of flow fields around an airfoil using MD-CNN-AE and examined the effects of three important hyperparameters [4]. Qu *et al.* applied a mode decomposition autoencoder using Variational Autoencoder (VAE) to cylinder flows at different Reynolds numbers [5]. Fukami *et al.* extended the hierarchical autoencoder proposed by Saegusa et al. [6] to apply to flow fields around two-dimensional cylinder and turbulent channel flows, extracting nonlinear modes of flow fields [7]. This method allows

mode decomposition considering the contribution of nonlinear modes to the reconstructed flow fields. Eivazi *et al.* extended the hierarchical CNN autoencoder using β-variational autoencoder to minimize the correlation of latent variables and constrain to satisfy orthogonality between modes, thereby extracting nonlinear modes with orthogonality from multi-scale turbulent flows [8].

In MD-CNN-AE models or mode decomposition models based on VAE, each decomposed flow field is obtained from each decoder. Hierarchical autoencoders comprise multiple subnetworks with encoders and decoders, resulting in decomposed flow fields from each subnetwork. When applying these methods to complex flows, particularly turbulence requiring numerous latent variables for flow reconstruction, the number of required modes increases, significantly increasing the number of model parameters and the learning costs. For example, in the case of applying POD to the velocity field of a flow around two parallel cylinders with a center-to-center distance of $1.5D$ and Reynolds number, $Re_D = U_\infty D/\nu = 100$, over 100 modes are needed to capture 99.9% of the kinetic energy. Applying a hierarchical autoencoder to the velocity field of turbulent channel flows with a friction Reynolds number $Re_\tau = 180$ requires two subnetworks with 144 modes to extract large-scale structures in wall turbulence. Thus, applying deep learning-based mode decomposition to complex flow fields based on existing methods can lead to increased learning costs in terms of computational performance and time, as well as potential overfitting. While decomposing into mode groups can reduce the number of model parameters and learning costs, understanding the phenomena of individual modes becomes difficult.

Therefore, to perform nonlinear mode decomposition of complex flow fields and enhancing our understanding of flow phenomena, this study proposes and constructs a deep learning model that reduces learning costs. We propose a Weight-sharing CNN Mode Decomposition Model (WS-MD model) by developing Murata *et al.*'s MD-CNN-AE model to reduce the number of layers and parameters within the model. This model enables the acquisition of multiple decomposed flow fields from a single common decoder that shares weights. The model is applied to a strong aperiodic flow around two parallel cylinders with a center-to-center distance of $2.0D$ and Reynolds number, $Re_D = U_\infty D/\nu = 100$, as an example of complex flows, and the characteristics of the decomposed flow fields are evaluated.

2 Datasets

To construct the training data, numerical simulations of two-dimensional flow around two parallel cylinders were performed using OpenFoam v2006. As shown in Figure 1, the computational domain was set to $24D \times 20D$, and two cylinders with equal diameters were arranged parallel to the flow $8D$ downstream from the inlet. Supradeepan and Roy conducted detailed numerical analysis on the effect of the spacing between the two cylinders on the characteristics of the flow around two parallel cylinders [9]. They reported that in parallel twin-cylinder flows with center-to-center distances between $1.4D$ and $2.2D$, the interaction of vortices shed from each cylinder is strong, showing a non-periodic pattern in the time series variation of drag and lift coefficients. In this study, rather than periodic flow fields

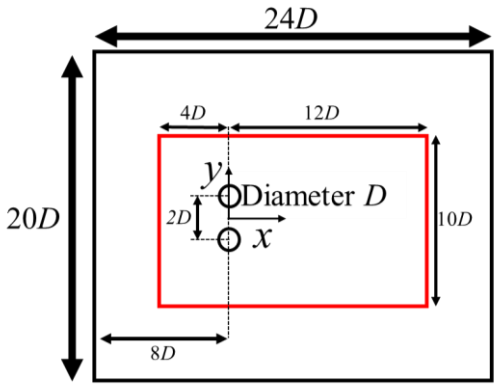

Fig. 1 Computational domain.

forming Kármán vortex streets around a single cylinder, we aim to decompose flow fields targeting non-periodic unsteady flows. Therefore, the center-to-center distance between the two cylinders is set to $2.0D$, and a dataset of complex unsteady flow fields with non-periodicity is constructed. The Reynolds number defined by the inlet velocity U_∞ and cylinder diameter D is set to $Re_D = U_\infty D/\nu = 100$. The PimpleFoam solver, combining the PISO and SIMPLE algorithms, is used for numerical simulations. All physical quantities presented hereafter are non-dimensionalized using the inlet velocity U_∞ and cylinder diameter D. The origin is set at the midpoint between the centers of the two cylinders, with the streamwise direction as x and the direction perpendicular to the streamwise (the spanwise direction) as y. A boundary-fitted grid system is used with the grids number of 79,872. The time step width for the numerical simulations is $\Delta t = 9.77 \times 10^{-2}$, and the total integration time after the flow has fully developed is $T = 781.6$.

From the flow field obtained by numerical simulation, velocity component in the streamwise direction, u, velocity component in the spanwise direction, v, and pressure p in the region surrounded by the red line in Figure 1 are extracted. To construct the final training data, two velocity components (u, v), and pressure (p) on the boundary-fitting grids are interpolated to 64×64 equally spaced grids, in the region surrounded by the red line. The time interval of the flow field in the training data corresponds to four times the time step of the numerical simulations, $\Delta t = 39.1 \times 10^{-2}$, with 2000 time steps of the flow field of velocities (u, v), and pressure (p) forming the spatial distribution of the training data set. Constructing a dataset with a long integration time with $T = 781.6$ and a time interval four times the numerical simulation time step is aimed at including the long-period fluctuations inherent in parallel twin-cylinder flow while reducing the cost required for training. The dimensions of the constructed input data are $N_x \times N_y \times N_v = 64 \times 64 \times 3$. N_x, N_y, and N_v represent the number of grid points in the x and y directions and the number of physical quantities (two velocity components and pressure) in the flow field, respectively. When performing mode decomposition of the flow field using a deep learning model, the input data matches the teacher data as the flow field is decomposed and then reconstructed. Also, the dimensions of the reconstructed flow field output by the model are the same as the input dimensions. Since the objective is to decompose the flow field into nonlinear modes, the 2000 sets of flow field data constructed are used both as training and validation data.

3 Deep Learning Model

To learn and extract spatial features of flow fields and perform nonlinear mode decomposition, a Mode Decomposition Convolutional Neural Network Autoencoder (MD-CNN-AE) based on Convolutional Neural Networks (CNN) and Autoencoders (AE) has been proposed and applied to flow field decomposition [3]. In this study, to perform nonlinear mode decomposition of complex flow fields, a deep learning model that reduces the number of model variables and learning costs is proposed: the Weight-sharing CNN Mode Decomposition Model (WS-MD model).

Figures 2(a) and 2(b) show the architecture diagrams of the MD-CNN-AE model and the WS-MD model, respectively. Both models are self-supervised autoencoders composed of an encoder and a decoder. In both models, flow field data representing the spatial distribution of mainstream velocity, u, spanwise velocity, v, and pressure, p, with $N_x \times N_y \times N_v = 64 \times 64 \times 3$ dimensions are provided as input. In the encoder, the instantaneous spatial distribution of the flow field with $64 \times 64 \times 3$ dimensions is compressed into a latent vector with $L_x \times L_y \times 1$ dimensions through convolutional processing, among others. The number of modes in the latent space is $L_x \times L_y = L$. Up to this point, the processes are common in both the MD-CNN-AE and WS-MD models. The processing in the decoder differs between the MD-CNN-AE model and the WS-MD model. In the MD-CNN-AE model, the latent vector with $L_x \times L_y \times 1$ dimensions is decomposed into L modes of $1 \times 1 \times 1$ dimensions. Each of the decomposed L modes is input into a separately constructed decoder. Next, each mode is decoded into a decomposed flow field with $64 \times 64 \times 3$ dimensions. Finally, the sum of the decomposed flow fields obtained by the decoders reconstructs the input flow field, which is output from

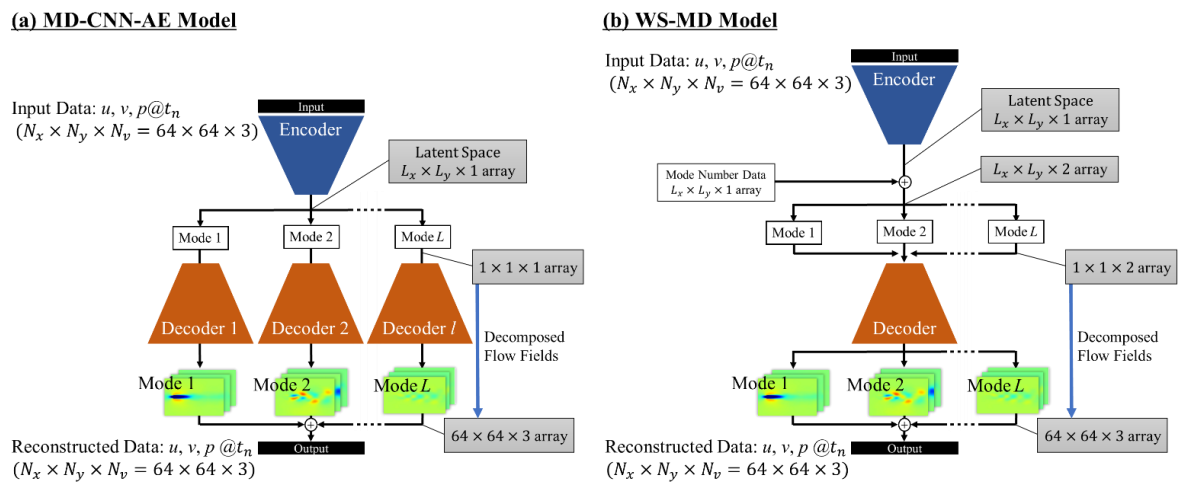

Fig. 2 Architectures of (a) the MD-CNN-AE model and (b) the Weight-sharing Mode Decomposition (WS-MD) model.

the model. Since each mode in the latent space produces a decomposed flow field, the number of decoders in the MD-CNN-AE model equals the number of modes, L. Therefore, when decomposing complex flow fields such as turbulence, the number of required decoders increases significantly, leading to increased learning costs. To reduce learning costs, instead of obtaining a decomposed flow field from each individual mode, each single decomposed flow field should be constructed from mode groups.

In contrast, the proposed WS-MD model avoids the increase in learning costs associated with the increase in the number of modes by sharing the decoder itself, including model variables, among multiple modes in the latent space while obtaining separate decomposed flow fields from each mode. The difference between the MD-CNN-AE and WS-MD models lies in the shared decoder and mode number labeling for each mode. In the WS-MD model's decoder, the latent vector with $L_x \times L_y \times 1$ dimensions is first concatenated with an array labeling the mode number for each mode. The latent vector with $L_x \times L_y \times 2 = L \times 2$ dimensions is then decomposed into L modes of $1 \times 1 \times 2$ dimensions. Each mode is expanded into a decomposed flow field by a single common decoder with completely shared model variables. Finally, the sum of the decomposed flow fields obtained by the decoder reconstructs the input flow field, which is output from the model. If the values of each mode obtained from the encoder are equal, the decomposed flow fields from the modes would be identical when using a single decoder with shared weights. To avoid such situations, the latent vector with $L_x \times L_y \times 1$ dimensions is labeled with mode numbers to explicitly distinguish each mode. When decomposing a flow field into L modes, the total number of parameters of the single shared decoder in the WS-MD model decreases to $1/L$ compared to the total number of parameters of L decoders in the MD-CNN-AE model.

In this paper, the WS-MD model with latent vector dimensions $(L_x,\ L_y) = (2, 2)$ and $(4, 4)$ is used for the nonlinear mode decomposition of a flow around two parallel cylinders. The number of modes in the latent space is $L = 4$ and 16, respectively, resulting in 4 and 16 decomposed flow fields.

4 Results

Two WS-MD models with $L = 4$ and 16 modes in the latent space were applied to the non-periodic strong a flow around two parallel cylinders with a center-to-center distance of $2.0D$ and Reynolds number, $Re_D = U_\infty D/\nu = 100$. The reconstructed flow fields and the flow fields decomposed into each mode by the learning models were evaluated. Here, the order of the modes is rearranged based on the kinetic energy of the decomposed flow fields from each mode obtained from the model.

In the WS-MD model with $L = 4$, the ratios of the kinetic energy of 1st to 4th modes are

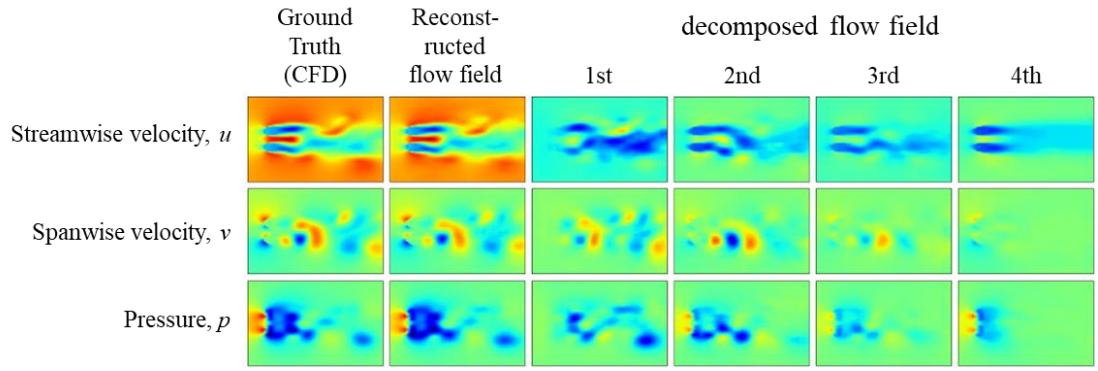

Fig. 3 Instantaneous distributions of the flow fields at t = 68.8: input (ground truth), the reconstruction, and decomposed flow fields obtained from the WS-MD model with 4 modes, for streamwise velocity u, spanwise velocity v, and pressure p.

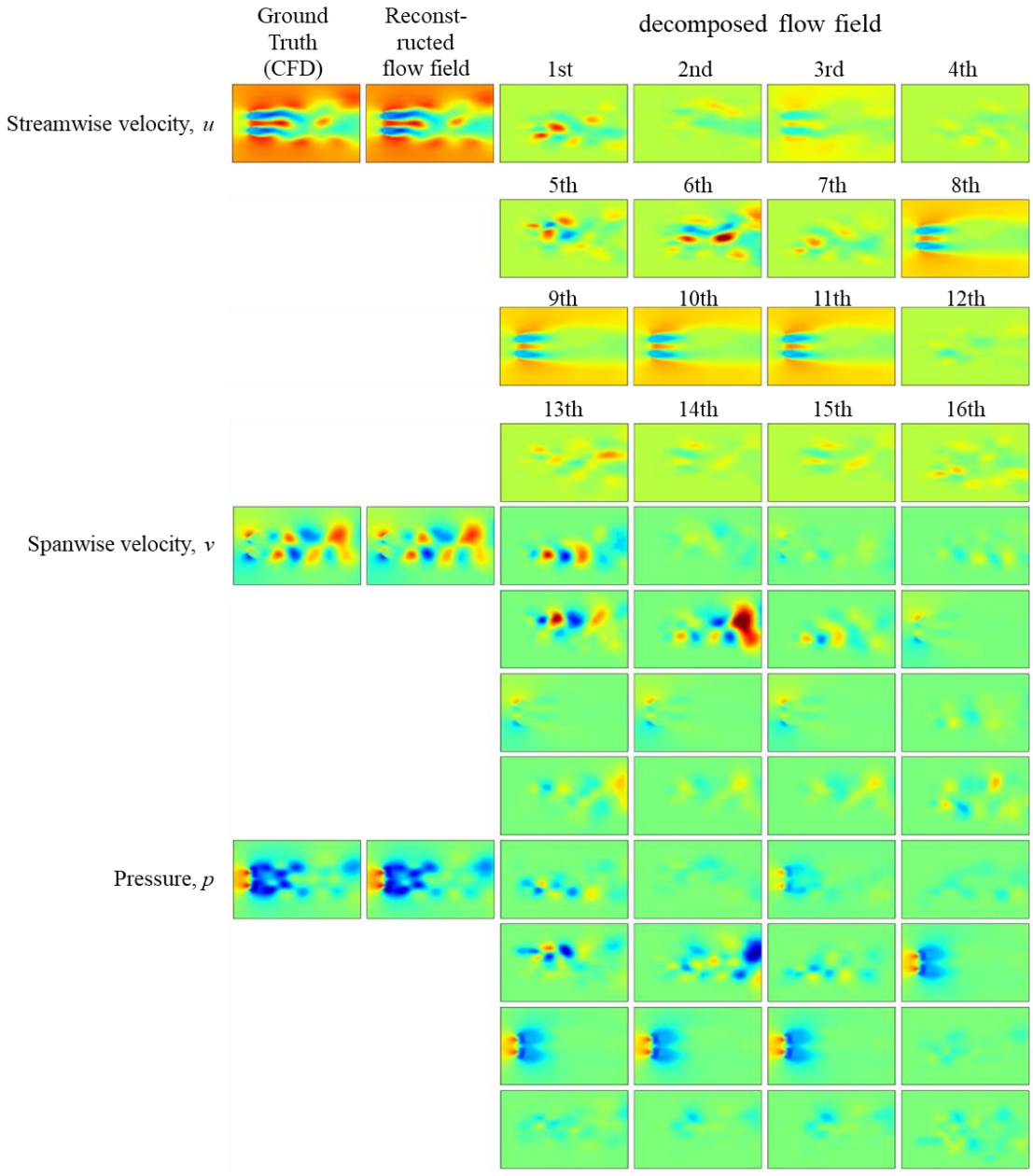

Fig. 4 Instantaneous distributions of the flow fields at t = 76.8: input (ground truth), the reconstruction, and decomposed flow fields obtained from the WS-MD model with 16 modes, for streamwise velocity u, spanwise velocity v, and pressure p.

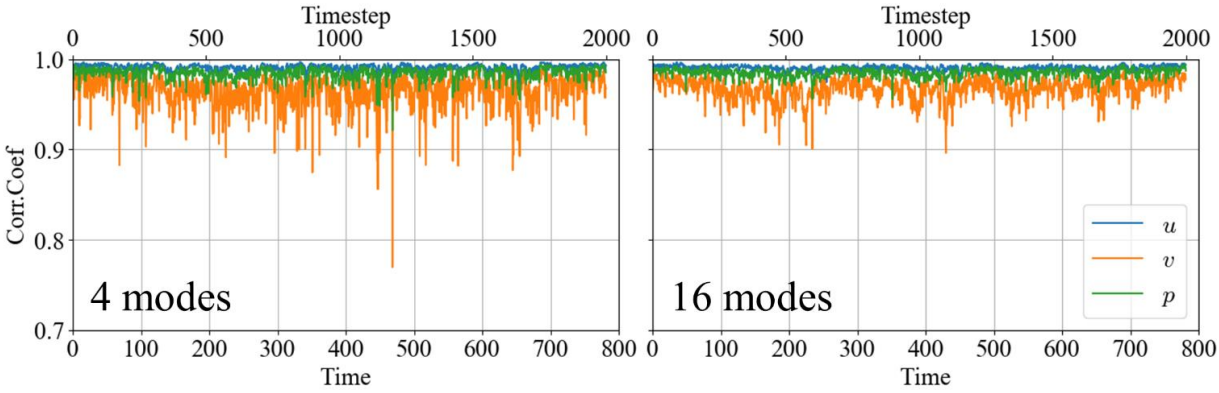

Fig. 5 Correlation coefficients of u, v and p, between the input and the output reconstructed by the WS-MD Models with 4 and 16 modes.

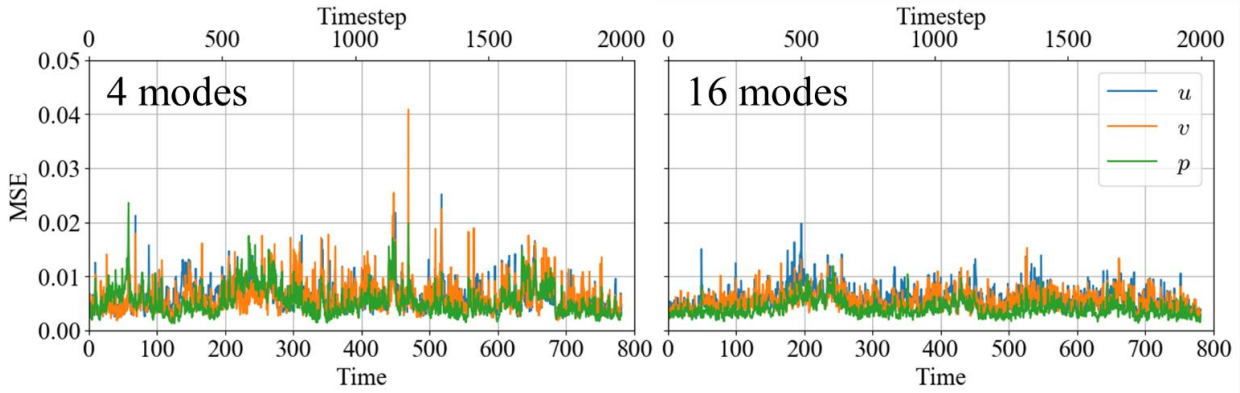

Fig. 6 MSEs of u, v and p, between the input and the output reconstructed by the WS-MD Models with 4 and 16 modes.

51.3: 21.6: 16.5: 10.6. In the WS-MD model with $L = 16$, the ratios of the kinetic energy of 1st to 16th modes are $18.8 : 17.1 : 14.2 : 13.3 : 9.05 : 4.46 : 3.89 : 2.84 : 2.84 : 2.84 : 2.84 : 2.64 : 1.97 : 1.20 : 1.20 : 0.79$. The sum of the kinetic energy of the decomposed flow fields does not match the kinetic energy of the reconstructed flow field. This discrepancy arises because the flow field decomposed, including the mean values, results in the average mode being dispersed across all decomposed flow fields, failing to satisfy orthogonality between modes.

Initially, the reconstructed flow fields from the two WS-MD models with $L = 4$ and 16 are evaluated. Figure 3 shows the flow fields of the CFD (i.e., the input data to the model, ground truth data), the reconstructed flow fields from the WS-MD model with $L = 4$, and the four decomposed flow fields, displaying the instantaneous spatial distribution of the streamwise velocity, u, spanwise velocity, v, and pressure, p. Figure 4 shows the CFD flow fields, the reconstructed flow fields from the WS-MD model with $L = 16$, and the 16 decomposed flow fields, displaying the instantaneous spatial distribution of velocity u, v, and pressure p. For both WS-MD models with $L = 4$ and 16, the reconstructed flow fields clearly reproduce the shedding of non-periodic vortices from the cylinders, showing good qualitative agreement with the CFD flow fields. Figure 5 shows the correlation coefficients between the flow fields reconstructed by the two WS-MD models with $L = 4$ and 16 and the CFD flow fields. For both models, the correlation coefficients for velocity u, v, and pressure p exceed 0.90 at most times. The WS-MD model with $L = 16$ showed slightly higher correlation coefficients overall compared to the model with $L = 4$. Figure 6 displays the MSEs (mean squared errors) between the flow fields reconstructed by both models and the CFD flow fields. The MSEs of u, v, and p are mostly below 0.02. Specifically, the MSE for the model with $L = 16$ is lower than that for the model with $L = 4$. From the perspectives of instantaneous spatial distributions, correlation coefficients, and MSEs, the flow fields reconstructed by the WS-MD model demonstrate strong qualitative and quantitative agreement with the CFD flow fields. The reconstruction performance of the model with $L = 16$ is superior to that of the model with $L = 4$. This relationship is consistent with the

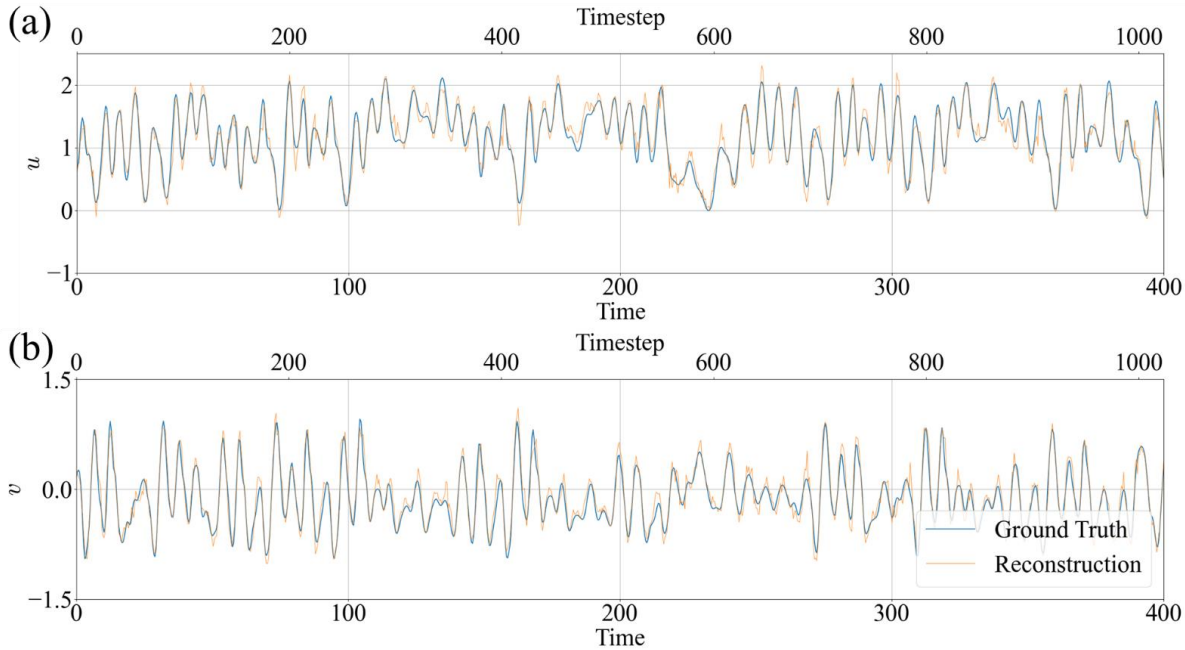

Fig.7 Time history of velocity from t = 0 to t = 400 at (x, y) = (1.50, 1.30) in the lower wake region for the ground truth (CFD) and reconstruction flow fields obtained from the WS-MD model with 4 modes: (a) streamwise velocity u, (b) spanwise velocity v.

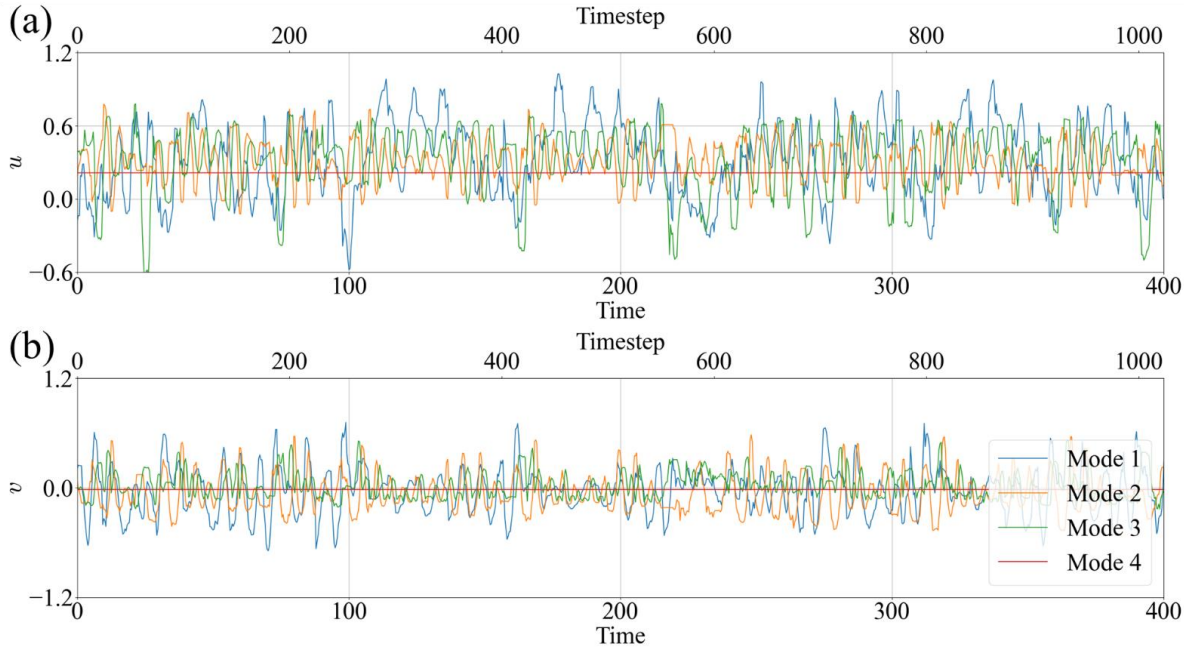

Fig. 8 Time history of velocity from $t = 0$ to $t = 400$ at $(x, y) = (1.50, 1.30)$ in the lower wake region for the four decomposed flow fields obtained from the WS-MD model with 4 modes: (a) streamwise velocity u, (b) spanwise velocity v.

general relationship between the number of modes and reconstruction accuracy.

Figure 7 shows the time series of velocity u, v at a downstream point $(x, y) = (1.50, 1.30)$ where multiple vortex structures generated from the lower cylinder pass. It compares the CFD flow fields with the flow fields reconstructed by the WS-MD model with $L = 4$. In the time series of the CFD flow fields, significant non-periodic fluctuations are observed. Despite the strong non-periodicity in the flow, the reconstructed flow fields exhibit good agreement with the CFD flow fields in both u and v. However, the high-frequency fluctuations observed in the CFD flow fields could not be accurately reconstructed.

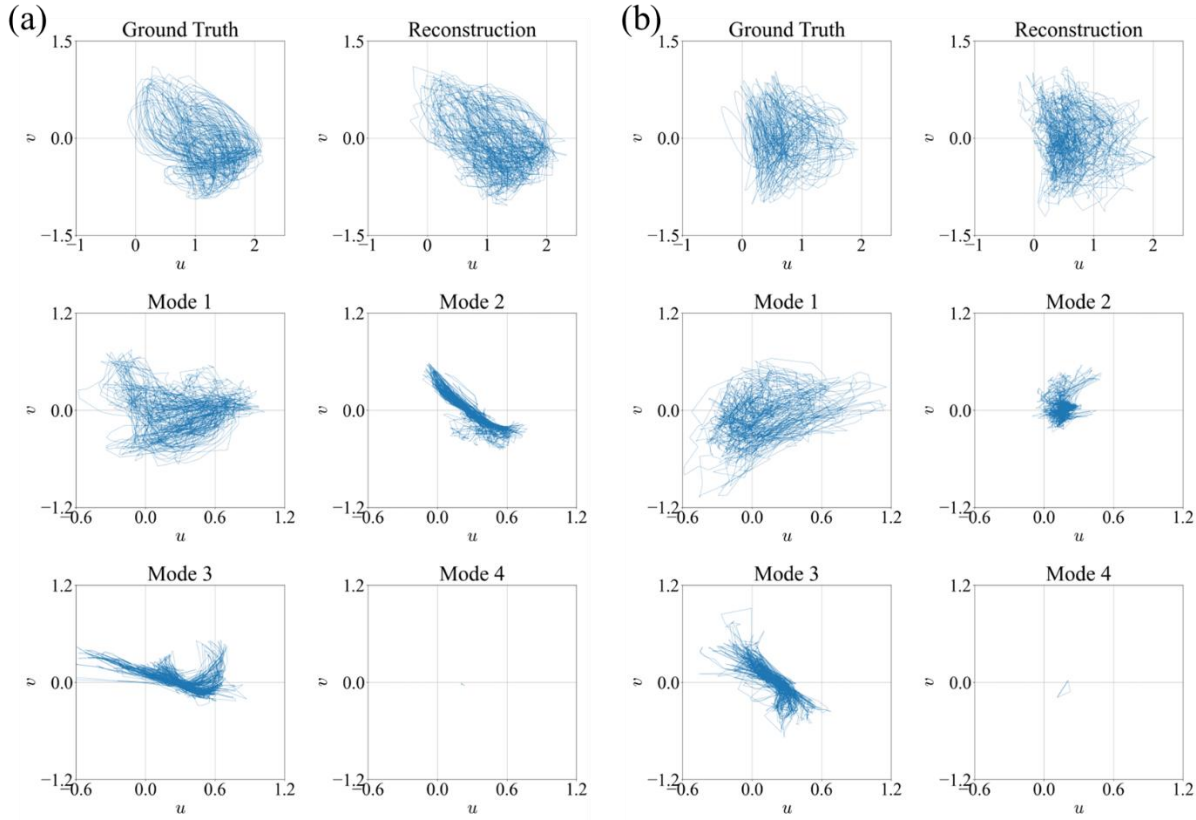

Fig. 9 Phase portraits of velocity u and v for ground truth, reconstruction and decomposition obtained by the WS-MD model with 4 modes: (a) at $(1.50, 1.30)$ in the lower wake region, and (b) at $(1.50, 1.95)$ in the upper wake region.

Tab. 1 Number of model parameters and average training time per epoch for the MD-CNN-AE Model and the WS-MD Model with 4 and 16 modes.

l	Model	Number of Model Parameters	Average Training Time per Epoch
4	MD-CNN-AE	846775	21.47 sec.
	WS-MD	217570	10.47 sec.
16	MD-CNN-AE	3363595	78.87 sec.
	WS-MD	217570	28.03 sec.

Next, the characteristics of the flow fields decomposed by the models with $L = 4$ and 16 are evaluated. Figure 3 shows the instantaneous spatial distribution of the flow fields decomposed by the model with $L = 4$. The flow fields decomposed into the 1st, 2nd, 3rd, and 4th modes exhibit distinct characteristics. The 1st mode shows unsteady vortex shedding from both the upper and lower cylinders with aperiodic behavior. In contrast, the 2nd and 3rd modes depict aperiodic fluctuations in vortex structures shed solely from the lower cylinder. These modes alternate in representing the vortex structures. The 4th mode displays a steady flow field similar to the time-averaged distribution observed in the CFD flow fields. Figure 4 illustrates the instantaneous spatial distribution of the flow fields decomposed by the model with $L = 16$. The decomposed flow fields in modes 8 to 11 are steady, resembling the time-averaged distribution of the CFD flow fields. The decomposed flow fields in the 1st to 7th and 12th to 16th modes are unsteady. Among the unsteady modes, the decomposed flow fields in the 1st, 2nd, 4th to 6th modes show large-scale unsteady structures corresponding to aperiodic vortices in the downstream region of the cylinders. In the reconstructed flow fields, vortex shedding is depicted by the periodic appearance and disappearance of vortices in these modes. The decomposed flow fields in the 3rd and 7th modes have structures of similar size and physical values in the

downstream region. Compared to the flow fields in the 1st, 2nd, 4th to 6th modes, the structures in the 3rd and 7th modes are smaller, with similar physical quantities. The flow fields in the 12th to 16th modes show smaller structures with lower physical values in the downstream region compared to the 1st to 7th modes. Note that the characteristics of each mode do not necessarily resemble each other even if their positional relationships in the latent space with $L_x \times L_y \times 1$ dimensions are close.

Figure 8 shows the time series of velocity u and v at a downstream point $(x, y) = (1.50, 1.30)$ where multiple vortex structures generated from the lower cylinder pass, comparing the four decomposed flow fields by the model with $L = 4$. The decomposed flow field in the 1st mode has the largest amplitude in both u and v. The amplitudes in the 2nd and 3rd modes are similar. The 4th mode exhibits constant temporal values. Figure 9 shows the phase portraits of velocity u and v at downstream points $(x, y) = (1.50, 1.30)$ and $(x, y) = (1.50, 1.95)$ comparing the CFD flow fields and the flow fields reconstructed or decomposed by the model with $L = 4$. Note that the range of values in the CFD flow fields, reconstructed flow fields, and decomposed flow fields varies. In the CFD flow fields, no periodicity resembling a steady circle is observed. This feature indicates that the flow around two parallel cylinders with a center-to-center distance of $2.0D$ at $Re = 100$ exhibits non-periodic behavior. The fluctuations in the reconstructed flow fields are close to those in the CFD flow fields. At the lower point $(x, y) = (1.50, 1.30)$, the decomposed flow field in the 1st mode exhibits non-periodic fluctuations. The decomposed flow fields in the 2nd and 3rd modes display periodic fluctuations, representing the aperiodic vortex structures shed from the lower cylinder. The steady decomposed flow field in the 4th mode shows very small fluctuations. The discrepancies between the non-periodic fluctuations in the reconstructed flow field and the sum of the 2nd to 4th modes is compensated by the 1st mode. At the upper point $(x, y) = (1.50, 1.95)$, the non-periodic fluctuations are represented by the decomposed flow fields in the 1st and 2nd modes. The decomposed flow field in the 3rd mode shows periodic fluctuations, while the 4th mode has very small fluctuations.

Finally, the evaluation focuses on the reduction in learning costs achieved by sharing the decoder. Table 1 presents the number of parameters of the MD-CNN-AE and WS-MD models with $L = 4$ and 16, along with the average learning time per iteration using one Nvidia Tesla V100 GPU. The number of parameters in the WS-MD model is reduced to 25.7% and 12.9% of the MD-CNN-AE model with $L = 4$ and 16, respectively. Additionally, the WS-MD model reduced the learning time to 48.8% and 35.6% compared to the MD-CNN-AE model with $L = 4$ and 16, respectively. The discrepancies between the reduction rate in learning time and the decrease in the number of model parameters are attributed to the processing of forward or backward propagation, which scales with the number of modes used for the shared decoder.

5 Conclusions

This study proposed a Weight-Sharing CNN Mode Decomposition Model (WS-MD model) by developing the MD-CNN-AE model to reduce the number of model variables and learning costs for nonlinear mode decomposition of complex unsteady flows using deep learning. The WS-MD model can extract multiple decomposed flow fields from a single common decoder that shares weights. Unlike conventional models where the decoder is not shared, the number of parameters in the decoder remains unchanged regardless of the number of modes. This results in reducing the computational cost of learning and inference processes as the number of modes increases.

The WS-MD model was applied to the strong aperiodic flow around two parallel cylinders with a center-to-center distance of $2.0D$ and Reynolds number, $Re_D = U_\infty D/\nu = 100$, as an example of unsteady flow, and the characteristics of the decomposed flow fields were evaluated. The characteristics of the reconstructed and decomposed flow fields were evaluated for two models with $L = 4$ and 16 modes in the latent space. From the perspectives of instantaneous spatial distribution, correlation coefficients, and MSE, the reconstructed flow fields showed very good quantitative agreement with the input flow fields. The decomposed flow fields obtained from the models exhibit

distinct characteristics. In the model with $L = 4$, three unsteady modes (1st, 2nd, and 3rd) and one steady mode (4th) were obtained. The 1st mode showed a non-periodic structure where vortex structures shed from the two cylinders interact. The 2nd and 3rd modes showed periodic fluctuations of vortex structures shed from the lower cylinder. The steady 4th mode showed a distribution similar to the time-averaged distribution of the CFD flow fields. In the model with $L = 16$, steady modes (8th to 11th) and other unsteady modes were obtained. The 1st, 2nd, and 4th to 6th modes showed large-scale unsteady structures corresponding to the vortex structures observed in the CFD flow fields downstream of the cylinders, represented by the periodic appearance and disappearance of vortices. These modes had larger physical values and structures compared to other unsteady modes. The steady 8th to 11th modes showed distributions close to the time-averaged distribution of the CFD flow fields.

The number of parameters of the shared decoder in the WS-MD model with L modes was reduced to $1/L$ compared to the number of parameters of L decoders in the MD-CNN-AE model. Consequently, the number of parameters in the WS-MD model was reduced to 25.7% and 12.9% of the MD-CNN-AE model with $L = 4$ and 16, respectively. Furthermore, in terms of learning time, the WS-MD model reduced the learning time to 48.8% and 35.6% compared to the MD-CNN-AE model with $L = 4$ and 16, respectively. The reduction in learning time did not match the decrease in the number of model parameters because of the execution of forward or backward propagation corresponding to the number of modes for the shared decoder.

These results demonstrated that the WS-MD model could extract decomposed flow fields with different characteristics from a single decoder. However, challenges remain in explaining and interpreting the physically decomposed flow fields by the deep learning model. Future tasks include establishing a nonlinear mode decomposition method that satisfies orthogonality while considering the kinetic energy and frequency characteristics of the flow fields. To address these challenges, we are advancing the construction of a Deterministic CNN Mode Decomposition Model (D-CNN-MD) that satisfies interpretability and orthogonality in nonlinear mode decomposition of flow fields using deep learning [12].

Acknowledgment

This work was partially supported by JSPS (Japan Society for the Promotion of Science): KAKENHI Grant Numbers 21H05007 and 22K03932.

References

[1] G. Berkooz, P. Holmes, and J. L. Lumley. The proper orthogonal decomposition in the analysis of turbulent flows. Annu. Rev. Fluid Mech., 25:539-575, 1993.
[2] P. J. Schmid. Dynamic mode decomposition of numerical and experimental data. J. Fluid Mech., 656:5-28, 2010.
[3] T. Murata, K. Fukami, and K. Fukagata. Nonlinear mode decomposition with convolutional neural networks for fluid dynamics. J. Fluid Mech., 882:13, 2020.
[4] X. Wu, S. Wu, X. Tian, X. Guo, and X. Luo. Effects of hyperparameters on flow field reconstruction around a foil by convolutional neural networks. Ocean Eng., 247:110650, 2022.
[5] J. Qu, W. Cai, and Y. Zhao. Deep learning method for identifying the minimal representations and nonlinear mode decomposition of fluid flows. Phys. Fluids, 33:103607, 2021.
[6] R. Saegusa, H. Sakano, and H. Hashimoto. Nonlinear principal component analysis to preserve the order of principal components. Neurocomputing, 61:57-70, 2004.
[7] K. Fukami, T. Nakamura, and K. Fukagata. Convolutional neural network based hierarchical autoencoder for nonlinear mode decomposition of fluid field data. Phys. Fluids, 32:095110, 2020.
[8] H. Eivazi, S. Le Clainche, S. Hoyas, and R. Vinuesa. Towards extraction of orthogonal and parsimonious non-linear modes from turbulent flows. Expert Syst. Appl., 202:117038, 2022.
[9] K. Supradeepan, and A. Roy. Characterisation and analysis of flow over two side by side cylinders

for different gaps at low Reynolds number: A numerical approach. Phys. Fluids, 26:063602, 2014.

[10] A. Krizhevsky, I. Sutskever, and G. E. Hinton. Imagenet classification with deep convolutional neural networks. Commun. ACM, 60:84-90, 2012.

[11] G. E. Hinton, and R. R. Salakhutdinov. Reducing the dimensionality of data with neural networks. Science, 313:504-507, 2006.

[12] Y. Shimoda, and N. Fukushima. CNN-based mode decomposition with deterministic latent space for unsteady flows. Proc. of AJK-FED 2023, 3-10-1-03, 2023.